






Long term measurement of the ^{87}Sr clock frequency at the limit of primary Cs clocks

R. Schwarz, S. Dörscher, A. Al-Masoudi, E. Benkler , T. Legero, U. Sterr , S. Weyers , J. Rahm ,
B. Lipphardt, and C. Lisdat *

Physikalisch-Technische Bundesanstalt, Bundesallee 100, 38116 Braunschweig, Germany



(Received 11 May 2020; accepted 20 July 2020; published 11 August 2020)

We report on a series of 42 measurements of the transition frequency of the 429 THz ($5s^2\ ^1S_0$ –($5s5p$) 3P_0) line in ^{87}Sr taken over three years from 2017 to 2019. They were performed at the Physikalisch-Technische Bundesanstalt (PTB) between the laboratory strontium lattice clock and the primary caesium fountain clocks CSF1 and CSF2. The length of each individual measurement run has been extended by use of a hydrogen maser as a flywheel to improve the statistical uncertainty given by the Cs clocks. We determine an averaged transition frequency of 429 228 004 229 873.00(0.07) Hz with 1.5×10^{-16} fractional uncertainty at the limit of the current realization of the unit hertz. Analysis of the data provides an improved limit on the coupling of the gravitational potential of the Sun to the proton-electron mass ratio μ and confirms the limits on the temporal drift of μ .

DOI: [10.1103/PhysRevResearch.2.033242](https://doi.org/10.1103/PhysRevResearch.2.033242)

I. INTRODUCTION

The revision of the International System of Units (SI) in 2019 marked a fundamental evolution in metrology. Several base units were redefined by assigning fixed values to fundamental constants [1,2]. While it is likely that no further redefinitions will be needed in the future to keep up with scientific progress for these units, the same is not the case for the most precisely realized unit so far, the SI unit “second” [3]. Redefining the second by fixing another fundamental constant (e.g., the electron mass m_e) is not constructive, because *ab initio* calculations of atomic transition frequencies from fundamental constants are by far not comparable in accuracy to present realizations. As progress in Cs clocks is saturating, and the reduction of the uncertainties of optical clocks—now in the low 10^{-18} range—is ongoing, a redefinition using optical atomic transitions is under discussion. The Consultative Committee for Time and Frequency (CCTF) of the Bureau International des Poids et Mesures (BIPM) issued a roadmap, defining requirements that optical clocks have to fulfill before a redefinition can take place [4]. Besides comparisons of optical clocks at the level of 10^{-18} and contributions of optical clocks to International Atomic Time (TAI), this roadmap also requires three independent measurements of optical clocks to independent Cs primary clocks with fractional uncertainty below 3×10^{-16} .

Even more fundamental, the base of all current precision measurements and the current SI is the assumption that fundamental constants are independent of space and time. In this respect, repeated measurements of the frequency ratios of clocks allow for tests of fundamental aspects of physics,

e.g., they probe for variations of the fine-structure constant α , the proton-electron mass ratio $\mu = m_p/m_e$, or the light quark mass to quantum chromodynamics mass scale ratio $X_q = m_q/\Lambda_{\text{QCD}}$ over time or as a function of position in a gravitational potential [5].

As optical frequency ratio measurements are mostly sensitive to variations of α , comparisons between optical clocks and clocks based on hyperfine transitions, like in absolute frequency measurements, play an important role for investigations concerning μ . Additionally, certain molecular transitions can be highly sensitive to variations of μ due to a cancellation between electronic and rovibrational energies [6–8]. Analysis of optical frequency ratios and absolute frequency measurements has therefore steadily lowered limits on the respective coupling coefficients and temporal drifts [9–17]. These investigations provide laboratory-based complements to astrophysical investigations on molecules [18,19].

In this article, we analyze 42 frequency measurements of the 429 THz transition ($5s^2\ ^1S_0$ –($5s5p$) 3P_0) in ^{87}Sr against PTB’s primary caesium fountain clocks CSF1 and CSF2 [20] accumulated over a period of three years. The data provide an improved value of the mean Sr transition frequency with 1.5×10^{-16} fractional uncertainty, the lowest one for an absolute frequency so far, fulfilling one of the requirements for a revision of the SI second. To exploit the performance of the Sr lattice clock with improved instability of $\sigma_{y,\text{Sr}} = 5 \times 10^{-17}/\sqrt{\tau}/\text{s}$, we employ a hydrogen maser as a flywheel oscillator to extend the 59 days total uptime of the Sr clock to about 120 days of comparison to the Cs clocks.

As a test of position invariance, the data were analyzed for annual variations due to the varying gravitational potential on the Earth’s elliptic orbit around the Sun. The amplitude of the corresponding fractional frequency variations amounts to $-18(86) \times 10^{-18}$. Disentangling the different possible contributions of varying fundamental constants using other measurements, we improve the limit on the coupling of the proton-electron mass ratio μ to a gravitational potential by a factor of 1.6, and we confirm the limits on its time dependence [17].

*christian.lisdat@ptb.de

II. FREQUENCY STANDARDS

The measurements described in this article involve three frequency standards, namely the Sr lattice clock and the two primary caesium fountain clocks CSF1 and CSF2. Active hydrogen masers serve as flywheel oscillators to bridge the downtimes of the optical frequency standard.

The Sr standard is located in a different building from the microwave frequency standards. The buildings are linked by path-length stabilized optical fibers and high-quality radio-frequency (rf) cables. The frequency conversion between optical and microwave domain can be performed in either building via optical frequency combs. Thus, either optical or microwave signals have to be exchanged between the buildings. The first is preferable as possible uncertainties, e.g., due to temperature-induced phase variations on the microwave cable, are minimized with shorter leads inside a single building. All frequencies are measured by dead time-free counters in phase-averaging (Λ) mode with a gate time of 1 s [21,22]. This mode allows for better phase noise suppression than frequency averaging (Π -mode), which, however, is of minor relevance for this work.

A. Sr lattice clock

The system has been described in detail previously [23–26]. Compared to the most recent uncertainty evaluation [26], two uncertainty contributions have been further reduced. The treatment of the lattice light shift has been changed and now employs an “operational magic wavelength” [27], reducing this contribution by a factor of 3. Secondly, we have more precisely taken into account the shift from blackbody radiation (BBR) emitted by the strontium oven on the atoms. For this characterization, a mechanical shutter located close to the oven was used to block radiation emitted into the vacuum chamber in one of two interleaved stabilizations of the interrogation laser to the atomic reference transition. These measurements allow for a much more accurate characterization of the light shift (by a factor of 8) than the previous geometry considerations [24]. The current uncertainty budget is shown in Table I. For most of the absolute frequency

TABLE I. Uncertainty budget of PTB’s laboratory Sr lattice clock. Corrections and uncertainties are given in fractional frequency units.

Effect	Correction (10^{-17})	Uncertainty $u_{b,Sr}$ (10^{-17})
Lattice light shift:	0.36	0.31
BBR, ambient:	490.64	1.37
BBR, oven:	0.30	0.12
Second-order Zeeman:	13.41	0.10
Collisions:	0.06	0.09
Servo error:	0.00	0.07
Tunnelling:	0.00	0.48
dc Stark shift:	0.20	0.07
Background gas collisions:	0.19	0.19
Other:	0.00	<0.01
Total:	505.2	1.5

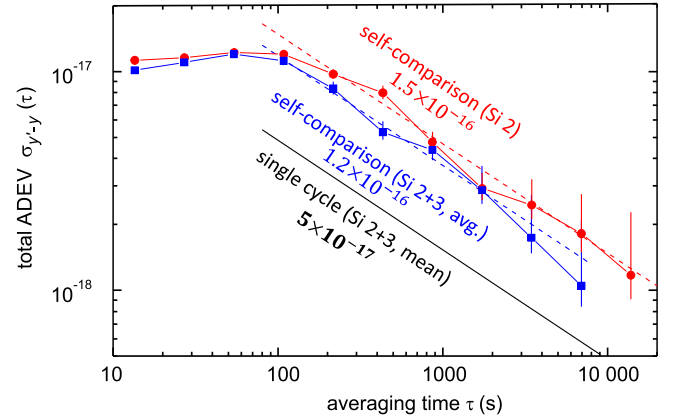


FIG. 1. Instabilities of the differential servo signals of two independent, interleaved servos running on the PTB Sr lattice clock using one cryogenic silicon cavity (Si 2) and averaging the frequency of two cavities (Si 2 + 3). We can infer an instability of the Sr frequency standard of $5 \times 10^{-17}/\sqrt{\tau/s}$ for a single stabilization (black line).

measurement intervals presented herein, the total uncertainty was higher but always remained below 3×10^{-17} .

The frequency instability of the Sr lattice clock has been improved by transferring the ultralow instability of a laser stabilized to a cryogenic Si cavity [28] to the 429 THz interrogation laser [29] of the Sr clock via an optical frequency comb [30,31]. The fractional frequency difference $y - y'$ between two interleaved stabilizations on the lattice clock exhibits a total Allan deviation (ADEV) of $\sigma_{y-y'} = 1.5 \times 10^{-16}/\sqrt{\tau/s}$ (Fig. 1). As we had access to two cryogenic cavities for some time, we were able to further reduce the laser noise by averaging the laser frequencies of two cavity-stabilized lasers by rf techniques in the stability transfer. The clock instability was thus reduced to $\sigma_{y-y'} = 1.2 \times 10^{-16}/\sqrt{\tau/s}$. All measurements were performed with a Rabi interrogation of 1.1 s length and a duty cycle of each interrogation of 66%.

If the full measurement time is dedicated to a single stabilization, we infer a fractional instability of the Sr frequency standard of $\sigma_{y,Sr} = 5 \times 10^{-17}/\sqrt{\tau/s}$ by applying the noise model presented in [25]. Dick effect-related noise and other noise sources contribute about equally to the clock instability. This result is on par with the currently best instabilities of optical clocks [32].

During frequency measurements, the Sr standard is usually operated including a dead time of 1 s to reduce the thermal load on the vacuum chamber caused by power dissipation in magnetic field coils. This increases the clock’s instability to $\sigma_{y,Sr} = (1 - 2) \times 10^{-16}/\sqrt{\tau/s}$, which is still well below the maser instability, but reduces the blackbody radiation uncertainty that dominates the systematic uncertainty $u_{b,Sr}$ (Table I).

B. Cs primary frequency standards

From 2017 to 2019, both caesium fountains CSF1 and CSF2 provided numerous calibrations of the scale unit of TAI. For this purpose, the fountains were running in primary frequency standard (PFS) mode [20], i.e., at the highest available level of accuracy, for several weeks. For the ^{87}Sr

TABLE II. Summary of the relevant information on the absolute frequency measurements for the respective measurement intervals labeled by the modified Julian date (MJD). $\Delta\nu$ is the value to be added to 429 228 004 228 000 Hz to get the frequency ν_{Sr} of the $(5s^2)^1S_0-(5s5p)^3P_0$ transition in ^{87}Sr measured by the fountain clocks CSF1 and CSF2, respectively. The statistical uncertainty contribution from the Sr frequency standard is below 1×10^{-18} for each measurement and therefore negligible. The total operation time of the Sr frequency standard is 59 days.

MJD (days)	T_{Sr} (s)	$u_{b,\text{Sr}}$ (10^{-16})	u_{ext}	CSF1					CSF2				
				T_{Cs} (days)	$u_{a,\text{Cs}}$ (10^{-16})	$u_{b,\text{Cs}}$	$\Delta\nu$ (Hz)	u (Hz)	T_{Cs} (days)	$u_{a,\text{Cs}}$ (10^{-16})	$u_{b,\text{Cs}}$	$\Delta\nu$ (Hz)	u (Hz)
57772	197 872	0.29	0.9						3.99	2.8	1.7	873.09	0.15
57779	186 418	0.28	3.0						2.13	3.3	1.7	872.95	0.21
57786	208 520	0.2	1.2						4.67	2.3	1.7	873.09	0.13
57870	143 640	0.25	1.4						4.11	2.6	1.7	872.97	0.15
58003	153 004	0.18	1.4						3.71	2.9	1.7	873.16	0.16
58232	377 157	0.2	0.8						7.66	1.7	1.7	873.06	0.11
58255	98 997	0.16	1.8						3.68	2.3	1.8	873.12	0.15
58283	230 162	0.17	1.1						5.33	2.0	1.8	872.93	0.12
58289	260 066	0.17	1.0	5.44	4.9	1.4	873.18	0.22	5.44	1.9	1.8	873.03	0.12
58304	194 721	0.17	1.2						5.21	1.9	1.8	873.09	0.12
58360	277 031	0.15	1.4	3.57	6.0	1.9	873.02	0.28	3.57	2.5	1.8	872.95	0.14
58380	67 635	0.2	2.3	3.62	5.6	1.7	873.16	0.27					
58388	99 503	0.25	1.9	2.88	6.6	1.4	872.72	0.30					
58396	107 452	0.21	1.7						3.55	6.2	1.7	873.37	0.29
58402	266 345	0.19	0.9						4.56	5.4	1.7	873.18	0.25
58409	336 176	0.16	0.8						5.11	4.9	1.7	873.38	0.22
58416	67 507	0.19	2.2						2.71	6.6	1.7	872.85	0.31
58444	289 470	0.2	0.9	5.67	5.1	1.5	872.57	0.23	5.54	2.2	1.7	873.13	0.13
58449	187 058	0.16	1.3	3.67	6.2	1.4	873.00	0.28	3.67	2.7	1.7	872.95	0.15
58505	68 058	0.18	2.2	2.78	7.2	1.4	872.87	0.33	2.78	3.1	1.7	873.23	0.18
58508	102 630	0.2	2.1	3.20	6.8	1.3	872.62	0.31	3.20	2.7	1.7	873.02	0.17
58513	110 455	0.19	1.9	3.49	6.7	1.9	873.45	0.31	3.49	2.9	1.7	873.24	0.17
58627	85 846	0.18	2.3	3.00	7.1	1.3	872.51	0.33	3.00	4.6	1.7	872.55	0.23
58661	177 461	0.16	1.4						4.93	2.6	1.7	872.99	0.15
58668	225 900	0.15	1.1						5.33	2.2	1.7	872.91	0.13
58675	265 248	0.19	1.0						5.67	2.2	1.7	873.16	0.13
58711	48 496	0.16	2.2	3.80	5.2	1.7	872.63	0.25	3.80	2.5	1.7	872.96	0.16
58750	59 726	0.17	2.2	3.17	6.3	2.3	873.30	0.30	3.17	3.1	1.7	872.97	0.18
58766	97 600	0.18	2.1	3.31	6.4	1.9	872.99	0.30	3.31	3.5	1.7	872.71	0.19
58771	126 282	0.16	1.6	3.56	5.7	1.6	873.01	0.26	3.56	2.9	1.7	873.19	0.16
Average							872.92	0.11				873.05	0.08

clock transition frequency measurements at hand, only data from such intervals have been evaluated. The comparison with TAI calibration data [33] from other primary and secondary frequency standards substantiates the performance of both fountains during the evaluation intervals.

In contrast to the typical PFS mode evaluations of CSF1 [20], we decided for the evaluations of the comparably short optical frequency measurement intervals to disentangle the statistical and systematic parts of the collisional shift evaluations by using collisional shift coefficients, which were obtained just in the actual measurement time. Like in CSF2, we include the statistical uncertainty of the individual collisional shift evaluations in the overall statistical uncertainty of the respective measurement intervals. As a result, the overall statistical uncertainties are largely ($\geq 95\%$) given by the statistical collisional shift uncertainties. Here, this treatment is advantageous, since the dominating type A part of the collisional shift uncertainty is reduced by the large number of short measurements. At the same time, the removal of the

type A part of the collisional shift uncertainty from the overall type B uncertainty results in lower systematic uncertainties (Table II) compared to the typical PFS mode evaluations of CSF1 [20]. The systematic uncertainties of CSF2 correspond to the previously published value [20]. Including the statistical uncertainty of the collisional shift evaluation, the effective ADEVs [20] are $\sigma_{y,\text{Cs}} = 3.3 \times 10^{-13}/\sqrt{\tau/s}$ and $\sigma_{y,\text{Cs}} = 1.6 \times 10^{-13}/\sqrt{\tau/s}$ for CSF1 and CSF2, respectively.

C. Hydrogen maser

During the period from 2017 through 2019, either of the active hydrogen masers H9 and H10 of the type VREMYA-CH VCH-1003M provided the rf reference at PTB. Their performance was constantly monitored by a cluster of masers. To evaluate the uncertainty introduced by the application of the maser as a flywheel oscillator in Sec. III, a maser noise model is required. It is based on the instability of the frequency ratio of the Sr standard and the respective maser

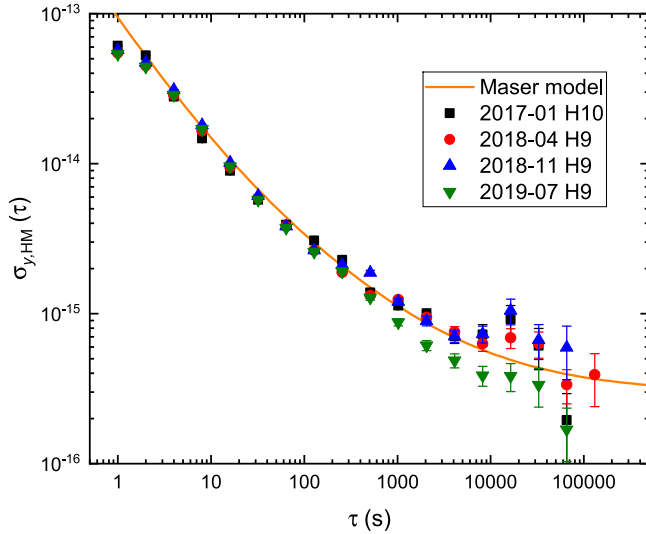


FIG. 2. Instabilities of the hydrogen masers H9 and H10 as determined by comparisons against the Sr lattice clock. Linear drifts of less than 1.1×10^{-16} per day were removed from the data.

from four long measurement intervals in January 2017, April 2018, November 2018, and July 2019. The ADEV shown in Fig. 2 was calculated under consideration of the gaps in the datasets [34] caused by the downtimes of the Sr clock or the optical frequency combs that are used to measure the frequency ratio. A linear frequency drift was removed from the data as the evaluation method in Sec. III is insensitive to it.

The fractional frequency instabilities shown in Fig. 2 are dominated by the maser noise as the optical frequency standard shows considerably better stability on all timescales. We model the single-sided power spectral density $S_y(f)$ of the maser by the power-law expansion $S_y = \sum_{\alpha=-1}^1 h_\alpha f^\alpha$ adding flicker frequency (FFN), white frequency (WFN), and flicker phase noise (FPN). The coefficients h_α are adjusted such that the calculated ADEV $\sigma_{y, HM}$ [22,35] matches the observations in Fig. 2. We find the coefficients

$$\begin{aligned} h_1 &= 4.3 \times 10^{-26} \text{ Hz}^{-2} \Rightarrow \sigma_{y, \text{FPN}} = 7 \times 10^{-14} \text{ s}/\tau, \\ h_0 &= 1.2 \times 10^{-27} \text{ Hz}^{-1} \Rightarrow \sigma_{y, \text{WFN}} = 2.4 \times 10^{-14} \sqrt{\text{s}/\tau}, \\ h_{-1} &= 6.5 \times 10^{-32} \Rightarrow \sigma_{y, \text{FFN}} = 3 \times 10^{-16}, \end{aligned} \quad (1)$$

using a cutoff frequency of 0.5 Hz.

III. DATA ANALYSIS AND RESULTS

Data from the Sr lattice clock were mainly recorded for other purposes than absolute frequency measurements. Therefore, they contain a relatively large number of gaps. Hence, the measurement intervals are often too short to achieve satisfactory statistical uncertainty in a direct comparison against a primary Cs clock. Applying the method described in [26], the results can be improved considerably: Due to the low instabilities of the masers and of the optical clock, in a first step their frequency ratio is evaluated with low statistical uncertainty on the intersection of uptimes of duration T_{Sr} of the optical clock, frequency comb, and links. We perform the

conversion from optical to microwave domain preferentially on the frequency comb located in the same building as the microwave standards (Sec. II). For intervals in which the Sr lattice clock was running, but neither of the optical links between the buildings was operational, we complemented the dataset by ratios measured via the microwave cable between the buildings, i.e., performing the conversion from microwave to optical domain at the frequency comb in the building with the lattice clock.

In a second step, the maser frequency is evaluated on a longer and uninterrupted time window of duration T_{Cs} by the primary frequency standards to lower the statistical uncertainty $u_{a, \text{Cs}} = \sigma_{y, \text{Cs}}(T_{\text{Cs}})$ related to the fountain clock. Combining both measurements gives an absolute frequency measurement of the Sr lattice clock against the caesium fountains with a statistical uncertainty lower than for a direct comparison without the maser as flywheel. As the maser frequency is averaged on two different measurement intervals, the respective averages $\bar{y}_i = \int y_i(t) g_i(t) dt$ with $i \in \{\text{Sr}, \text{Cs}\}$ are not necessarily equal. The weighting function $g_i(t)$ is $1/T_i$ during the uptime of the respective clock and zero otherwise, where T_i denotes the total operation time of clock i . Therefore, an extrapolation uncertainty $u_{\text{ext}}^2 = \langle (\bar{y}_{\text{Sr}} - \bar{y}_{\text{Cs}})^2 \rangle$ must be included that reflects this unknown. It is calculated from the well-characterized single-sided power spectral density $S_y(f)$ of the flywheel oscillator (Sec. II) by applying Parseval's theorem. We find [26]

$$u_{\text{ext}}^2 = \int_0^\infty S_y(f) |G(f)|^2 df \quad (2)$$

with $G(f) = \int [g_{\text{Sr}}(t) - g_{\text{Cs}}(t)] \exp(-2\pi i f t) dt$. Note that this approach is insensitive to linear drifts of the flywheel's frequency if the centers of gravity of both g_i coincide. Otherwise, drift correction has to be applied. Here, the centers of gravity deviate for some measurement intervals by a few hours. As the frequency drift of the masers is below 1.1×10^{-16} per day, the correction and its uncertainty contribution are negligible.

As discussed in [26], the statistical uncertainty of such a measurement is $u_a^2 = u_{\text{ext}}^2 + \sigma_{y, \text{Sr}}^2(T_{\text{Sr}}) + \sigma_{y, \text{Cs}}^2(T_{\text{Cs}})$, where the second term is negligibly small in our measurements. We have investigated at which T_{Cs} the combined statistical uncertainty u_a is minimized for each measurement window. The length of filled gaps was restricted to a maximum of one day. We find that for any individual measurement, the value of u_a is only weakly dependent on the choice of T_{Cs} . Information on measurement intervals including dataset lengths, uncertainties, and the measured frequencies of the Sr clock are summarized in Table II. Figure 3 shows the measured absolute frequencies ν_{Sr} .

The statistical uncertainty $u_{a, \text{Cs}}$ is, like the small statistical uncertainty contribution from the Sr frequency standard and u_{ext} (to a very large extent), uncorrelated between the measurement windows. As the systematic uncertainties u_b of the frequency standards, in particular of CSF1, vary throughout the dataset for each fountain, weighted averages taking into account correlated (u_b) and uncorrelated (u_a, u_{ext}) uncertainty contributions are calculated [36]. We find the frequency values and uncertainties given in the last line of Table II. The uncertainties are 2.4×10^{-16} and 1.9×10^{-16} in

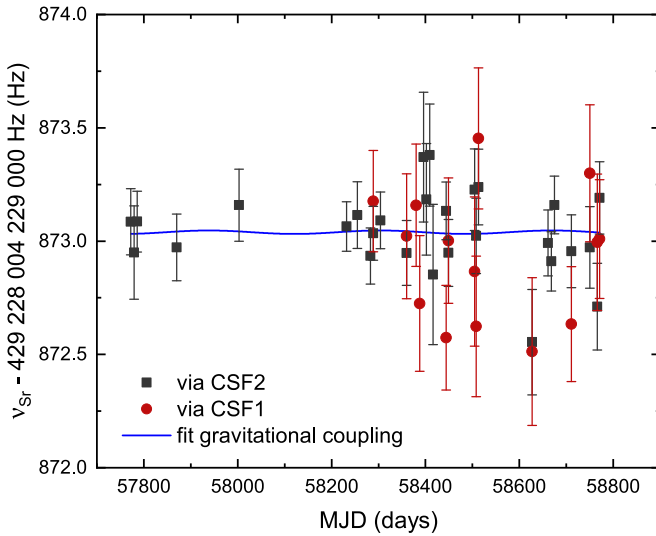


FIG. 3. Absolute frequencies ν_{Sr} of the $(5s^2) ^1S_0 - (5s5p) ^3P_0$ transition in ^{87}Sr measured by the Cs fountain clocks CSF1 and CSF2. Modified Julian dates (MJD), frequencies, and uncertainties u from Table II. The curve shows the fit to obtain limits on the coupling μ to the gravitational potential of the Sun (Sec. IV).

fractional frequency units for CSF1 and CSF2, respectively. Considering the systematic uncertainties of both fountain clocks as uncorrelated and neglecting the small correlations introduced by u_{ext} for windows with measurements by both fountains, we calculate a weighted average frequency of 429 228 004 229 873.00(0.07) Hz. The fractional frequency uncertainty of 1.5×10^{-16} is even slightly below the record one reached for an Yb lattice clock [17]. These results are in very good agreement with the numerous previous determinations of ν_{Sr} by a variety of groups [13,23,24,26,37–51] (Fig. 4) and the value for ν_{Sr} recommended as a secondary representation of the second [52].

IV. GRAVITATIONAL COUPLING AND DRIFT OF m_p/m_e

Extended datasets of accurate clock comparisons have been analyzed to test our understanding of physics. Typically, a possible violation of the Einstein equivalence principle (EEP) is investigated that would manifest itself as drift or modulation of the measured frequency ratio. A violation may be caused by temporal variations of fundamental constants or their coupling to a gravitational potential [9,11–17,53]. We first investigate the data in Table II with respect to a coupling of the proton-electron mass ratio μ to the gravitational potential of the Sun. In the second part of this section, we address a possible temporal variation $\dot{\mu}$ on an extended dataset.

A coupling of the Sr/Cs frequency ratio to the Sun's gravitational potential would cause a modulation of ν_{Sr} of

$$\nu_{\text{Sr}}(t) = \nu_0 [1 + A \cos [2\pi(t - t_0)/T_0]] \quad (3)$$

with $T_0 \approx 365.260$ days (the duration of the anomalistic year). For this analysis, t_0 is the perihelion of 2018. Fitting this expression to the data, we find $A = -18(86) \times 10^{-18}$. We

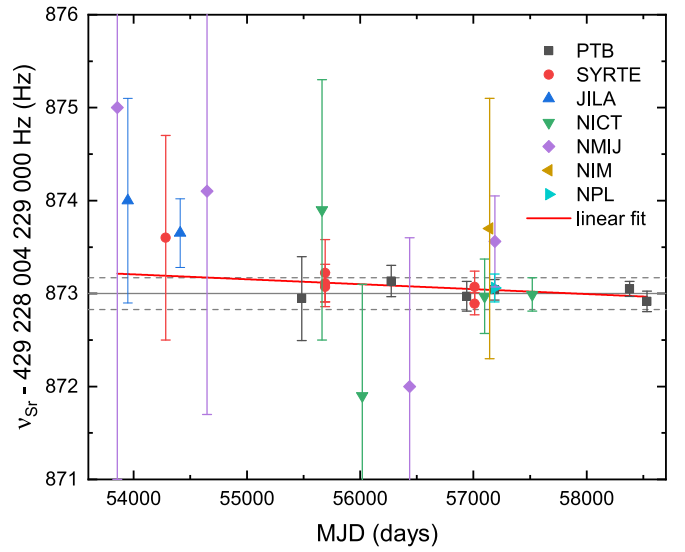


FIG. 4. Overview of the measured values of the ^{87}Sr 429 THz transition. The two squares on the right show the average values from Table II. The horizontal gray line shows the value of the frequency recommended as a secondary representation of the second (dashed lines: uncertainty). The red line is a fit to derive $\dot{\mu}/\mu$.

treated the uncertainties of all $\Delta\nu$ in Table II as uncorrelated. Although this approach neglects correlations in the respective uncertainties introduced by, for instance, contributions to u_b from, e.g., atomic parameters that are common for all measurements, this only causes an overestimation of the uncertainty of the fit parameter A . The reduced χ^2 of 1.3 of the fit indicates that the fit is statistically well behaved. With annual variation of the gravitational potential $\Delta\Phi = (\Phi_{\text{max}} - \Phi_{\text{min}})/2 \approx 1.65 \times 10^{-10}c^2$ (c being the speed of light in vacuum), we find the coupling coefficient

$$\beta_{\text{Sr,Cs}} = \frac{A}{\Delta\Phi/c^2} = -1.1(5.2) \times 10^{-7}, \quad (4)$$

thus no violation of the EEP is found. The limit set by our data is about a factor of 2 less stringent than the ones set by Ashby *et al.* [16] or Dzuba and Flambaum [53]. In principle, our data could be supplemented as in [17] by measurements performed by other groups, but the exact measurement intervals and their individual frequency values of past measurements are often not reported, which is why we refrain from this approach.

Effects causing a violation of EEP could be variations of the fine-structure constant α , of the ratio of light quark mass to the quantum chromodynamics (QCD) scale $X_q = m_q/\Lambda_{\text{QCD}}$, or of μ . For each effect and pair of compared clocks X, Y , sensitivity coefficients $\Delta K_\epsilon(X, Y) = d \ln(\nu_X/\nu_Y)/d \ln(\epsilon)$ with $\epsilon \in \{\alpha, X_q, \mu\}$ have been determined through atomic and nuclear structure calculations [54,55]. For the pair (Sr,Cs) these calculations yield $\Delta K_\alpha(\text{Sr}, \text{Cs}) = -2.77$, $\Delta K_{X_q}(\text{Sr}, \text{Cs}) = -0.002$, and $\Delta K_\mu(\text{Sr}, \text{Cs}) = 1$. Thus the coupling to the gravitational potential can be expressed as $\beta_{\text{Sr,Cs}} = \sum_\epsilon \Delta K_\epsilon(\text{Sr}, \text{Cs}) k_\epsilon$ with species-independent coupling coefficients $k_\epsilon = d \ln(\epsilon)/d(\Phi/c^2)$ for the respective effects.

Using limits on the other parameters' variations from complementary investigations as in [17], $k_\alpha = 0.54(1.02) \times$

10^{-7} [53] from the Al^+/Hg^+ frequency ratio, which is only sensitive to variations of α , and $k_{X_q} = -2.6(2.6) \times 10^{-6}$ from the H,Cs pair [16], we derive a refined coupling parameter k_μ from our $\beta_{\text{Sr,Cs}}$ [Eq. (4)]:

$$k_\mu = 3.5(5.9) \times 10^{-7}. \quad (5)$$

This result is a factor of 1.6 more stringent than the result by McGrew *et al.* [17] for the combined data of Yb and Sr lattice clocks.

To analyze our data for temporal variation $\dot{\mu}/\mu$, we combine them with previously published values of ν_{Sr} [13,23,24,26,39–51,56], spanning in total more than 12 years. We use the averaged frequency values only and estimate, where necessary, the time of measurement, whose exact knowledge is of smaller relevance for this analysis than for the one above. Where averaged frequency values from measurements against different fountain clocks are available in a publication, we use those instead of the combined averages. Fitting a linear temporal variation of ν_{Sr} (Fig. 4) yields a slope of $\dot{\nu} = -4.2(3.3) \times 10^{-17}/\text{a}$ in fractional frequency units. This result slightly improves on the limit given in [17] of $-4.9(3.6) \times 10^{-17}/\text{a}$ that is based on Yb lattice clock data in addition to the same published Sr frequency measurements.

Expressing the variation $\dot{y} = \sum_i \Delta K_\epsilon(X, Y) d \ln(\epsilon)/dt$ as a sum of three varying fundamental constants $\epsilon \in \{\alpha, X_q, \mu\}$, and restricting two of them by published values $\dot{X}_q/X_q = 0.14(9) \times 10^{-16}/\text{a}$ from [11] and the averaged value from [14,15] $\dot{\alpha}/\alpha = -1.4(2.0) \times 10^{-17}/\text{a}$ (as both results are probably strongly correlated, we have kept the slightly lower uncertainty from [15]), we obtain

$$\dot{\mu}/\mu = -6.9(6.5) \times 10^{-17}/\text{a}. \quad (6)$$

This value confirms the rate $\dot{\mu}/\mu = -5.2(6.5) \times 10^{-17}/\text{a}$ found in [17] obtained from Sr and Yb lattice clock frequency measurements. It is interesting to note that the uncertainty of both results is limited by that of $\dot{\alpha}/\alpha$ [14,15].

V. CONCLUSION

We have presented more than 40 measurements of the ^{87}Sr 429 THz clock transition against PTB's primary fountain clocks CSF1 and CSF2. The uncertainty of the average frequency is 65 mHz (1.5×10^{-16} in fractional units), which is more accurate than the best absolute frequency measurements so far [13,15,17,26,56,57]. Our result is a valuable contribution to the validation of ^{87}Sr lattice clocks as a secondary representation of the second as well as to a future redefinition of the SI unit second.

We have presented an updated uncertainty budget of PTB's Sr lattice clock at a fractional uncertainty level of 1.5×10^{-17} . Self-comparisons of two clock stabilization cycles run on the same apparatus indicate that our lattice clock can reach an instability of $\sigma_{y,\text{Sr}} = 5 \times 10^{-17}/\sqrt{\tau}/\text{s}$, a level similar to the one reached in [32].

Using the frequency comparisons between Cs and Sr clocks, we have performed a test of the Einstein equivalence principle that—in combination with data from [16,53]—allows us to put more a stringent limit on the coupling constant between the proton-electron mass ratio μ and a gravitational potential of $k_\mu = 3.5(5.9) \times 10^{-7}$. The limit we set on $\dot{\mu}/\mu = -6.9(6.5) \times 10^{-17}/\text{a}$ confirms the result given in [17].

ACKNOWLEDGMENTS

We acknowledge support by the project 18SIB05 ROCIT, which has received funding from the EMPIR programme cofinanced by the Participating States and from the European Union's Horizon 2020 research and innovation programme, and by the Deutsche Forschungsgemeinschaft (DFG, German Research Foundation) under Germany's Excellence Strategy—EXC-2123 Quantum Frontiers—390837967 and CRC 1228 DQ-mat within project B02. This work was partially supported by the Max Planck-RIKEN-PTB Center for Time, Constants and Fundamental Symmetries. We acknowledge the fruitful collaboration with Jun Ye's group at JILA, Boulder in the development of cryogenic silicon resonators.

-
- [1] Bureau International des Poids et Mesures, *Le Système international d'unités/The International System of Units*, 9th ed. (BIPM, Sèvres, 2019), online at <https://www.bipm.org/utlis/common/pdf/si-brochure/SI-Brochure-9.pdf>
- [2] E. O. Göbel and U. Siegener, *The New International System of Units (SI)* (Wiley-VCH, Berlin, 2019).
- [3] S. Bize, *C. R. Phys.* **20**, 153 (2019).
- [4] F. Riehle, P. Gill, F. Arias, and L. Robertsson, *Metrologia* **55**, 188 (2018).
- [5] V. V. Flambaum, *J. Mod. Phys. A* **22**, 4937 (2007).
- [6] V. V. Flambaum and M. G. Kozlov, *Phys. Rev. Lett.* **99**, 150801 (2007).
- [7] J. Bagdonaite, P. Jansen, C. Henkel, H. L. Bethlem, K. M. Menten, and W. Ubachs, *Science* **339**, 46 (2013).
- [8] J. Kobayashi, A. Ogino, and S. Inouye, *Nat. Commun.* **10**, 3771 (2019).
- [9] T. Rosenband, D. B. Hume, P. O. Schmidt, C. W. Chou, A. Brusch, L. Lorini, W. H. Oskay, R. E. Drullinger, T. M. Fortier, J. E. Stalnaker, S. A. Diddams, W. C. Swann, N. R. Newbury, W. M. Itano, D. J. Wineland, and J. C. Bergquist, *Science* **319**, 1808 (2008).
- [10] S. Blatt, A. D. Ludlow, G. K. Campbell, J. W. Thomsen, T. Zelevinsky, M. M. Boyd, J. Ye, X. Baillard, M. Fouché, R. L. Targat, A. Brusch, P. Lemonde, M. Takamoto, F. L. Hong, H. Katori, and V. V. Flambaum, *Phys. Rev. Lett.* **100**, 140801 (2008).
- [11] J. Guéna, M. Abgrall, D. Rovera, P. Rosenbusch, M. E. Tobar, P. Laurent, A. Clairon, and S. Bize, *Phys. Rev. Lett.* **109**, 080801 (2012).
- [12] S. Peil, S. Crane, J. L. Hanssen, T. B. Swanson, and C. R. Ekstrom, *Phys. Rev. A* **87**, 010102 (2013).
- [13] R. Le Targat, L. Lorini, Y. Le Coq, M. Zawada, J. Guéna, M. Abgrall, M. Gurov, P. Rosenbusch, D. G. Rovera, B. Nagórny, R. Gartman, P. G. Westergaard, M. E. Tobar, M. Lours, G. Santarelli, A. Clairon, S. Bize, P. Laurent, P. Lemonde, and J. Lodewyck, *Nat. Commun.* **4**, 2109 (2013).

- [14] R. M. Godun, P. B. R. Nisbet-Jones, J. M. Jones, S. A. King, L. A. M. Johnson, H. S. Margolis, K. Szymaniec, S. N. Lea, K. Bongs, and P. Gill, *Phys. Rev. Lett.* **113**, 210801 (2014).
- [15] N. Huntemann, B. Lipphardt, C. Tamm, V. Gerginov, S. Weyers, and E. Peik, *Phys. Rev. Lett.* **113**, 210802 (2014).
- [16] N. Ashby, T. E. Parker, and B. R. Patla, *Nat. Phys.* **14**, 822 (2018).
- [17] W. F. McGrew, X. Zhang, H. Leopardi, R. J. Fasano, D. Nicolodi, K. Beloy, J. Yao, J. A. Sherman, S. A. Schäffer, J. Savory, R. C. Brown, S. Römisch, C. W. Oates, T. E. Parker, T. M. Fortier, and A. D. Ludlow, *Optica* **6**, 448 (2019).
- [18] W. Ubachs, J. Bagdonaite, E. J. Salumbides, M. T. Murphy, and L. Kaper, *Rev. Mod. Phys.* **88**, 021003 (2016).
- [19] W. Ubachs, *Space Sci. Rev.* **214**, 3 (2018).
- [20] S. Weyers, V. Gerginov, M. Kazda, J. Rahm, B. Lipphardt, G. Dobrev, and K. Gibble, *Metrologia* **55**, 789 (2018).
- [21] G. Kramer and W. Klische, Extra high precision digital phase recorder, in *Proceedings of the 18th European Frequency and Time Forum, Guildford, UK* (IET, London, 2004), pp. 595–602.
- [22] E. Benkler, C. Lisdat, and U. Sterr, *Metrologia* **52**, 565 (2015).
- [23] S. Falke, H. Schnatz, J. S. R. Vellere Winfred, T. Middelman, S. Vogt, S. Weyers, B. Lipphardt, G. Grosche, F. Riehle, U. Sterr, and C. Lisdat, *Metrologia* **48**, 399 (2011).
- [24] S. Falke, N. Lemke, C. Grebing, B. Lipphardt, S. Weyers, V. Gerginov, N. Huntemann, C. Hagemann, A. Al-Masoudi, S. Häfner, S. Vogt, U. Sterr, and C. Lisdat, *New J. Phys.* **16**, 073023 (2014).
- [25] A. Al-Masoudi, S. Dörscher, S. Häfner, U. Sterr, and C. Lisdat, *Phys. Rev. A* **92**, 063814 (2015).
- [26] C. Grebing, A. Al-Masoudi, S. Dörscher, S. Häfner, V. Gerginov, S. Weyers, B. Lipphardt, F. Riehle, U. Sterr, and C. Lisdat, *Optica* **3**, 563 (2016).
- [27] H. Katori, V. D. Ovsianikov, S. I. Marmo, and V. G. Palchikov, *Phys. Rev. A* **91**, 052503 (2015).
- [28] D. G. Matei, T. Legero, S. Häfner, C. Grebing, R. Weyrich, W. Zhang, L. Sonderhouse, J. M. Robinson, J. Ye, F. Riehle, and U. Sterr, *Phys. Rev. Lett.* **118**, 263202 (2017).
- [29] S. Häfner, S. Falke, C. Grebing, S. Vogt, T. Legero, M. Merimaa, C. Lisdat, and U. Sterr, *Opt. Lett.* **40**, 2112 (2015).
- [30] C. Hagemann, C. Grebing, T. Kessler, S. Falke, N. Lemke, C. Lisdat, H. Schnatz, F. Riehle, and U. Sterr, *IEEE Trans. Instrum. Meas.* **62**, 1556 (2013).
- [31] E. Benkler, B. Lipphardt, T. Puppe, R. Wilk, F. Rohde, and U. Sterr, *Opt. Express* **27**, 36886 (2019); see also erratum [58].
- [32] E. Oelker, R. B. Hutson, C. J. Kennedy, L. Sonderhouse, T. Bothwell, A. Goban, D. Kedar, C. Sanner, J. M. Robinson, G. E. Marti, D. G. Matei, T. Legero, M. Giunta, R. Holzwarth, F. Riehle, U. Sterr, and J. Ye, *Nat. Photonics* **13**, 714 (2019).
- [33] BIPM Circular T monthly, available at <http://www.bipm.org/jsp/en/TimeFtp.jsp>.
- [34] I. Sesia and P. Tavella, *Metrologia* **45**, S134 (2008).
- [35] S. T. Dawkins, J. J. McFerran, and A. N. Luiten, *IEEE Trans. Ultrason. Ferroelectr. Freq. Control* **54**, 918 (2007).
- [36] G. Cowan, *Statistical Data Analysis* (Oxford Science Publications, Clarendon, 1998).
- [37] A. D. Ludlow, M. M. Boyd, T. Zelevinsky, S. M. Foreman, S. Blatt, M. Notcutt, T. Ido, and J. Ye, *Phys. Rev. Lett.* **96**, 033003 (2006).
- [38] R. Le Targat, X. Baillard, M. Fouché, A. Brusch, O. Tcherbakoff, G. D. Rovera, and P. Lemonde, *Phys. Rev. Lett.* **97**, 130801 (2006).
- [39] M. Takamoto, F. L. Hong, R. Higashi, Y. Fujii, M. Imae, and H. Katori, *J. Phys. Soc. Jpn.* **75**, 104302 (2006).
- [40] M. M. Boyd, A. D. Ludlow, S. Blatt, S. M. Foreman, T. Ido, T. Zelevinsky, and J. Ye, *Phys. Rev. Lett.* **98**, 083002 (2007).
- [41] X. Baillard, M. Fouché, R. Le Targat, P. G. Westergaard, A. Lecallier, F. Chapelet, M. Abgrall, G. D. Rovera, P. Laurent, P. Rosenbusch, S. Bize, G. Santarelli, A. Clairon, P. Lemonde, G. Grosche, B. Lipphardt, and H. Schnatz, *Eur. Phys. J. D* **48**, 11 (2008).
- [42] G. K. Campbell, A. D. Ludlow, S. Blatt, J. W. Thomsen, M. J. Martin, M. H. G. de Miranda, T. Zelevinsky, M. M. Boyd, J. Ye, S. A. Diddams, T. P. Heavner, T. E. Parker, and S. R. Jefferts, *Metrologia* **45**, 539 (2008).
- [43] F. L. Hong, M. Musha, M. Takamoto, H. Inaba, S. Yanagimachi, A. Takamizawa, K. Watabe, T. Ikegami, M. Imae, Y. Fujii, M. Amemiya, K. Nakagawa, K. Ueda, and H. Katori, *Opt. Lett.* **34**, 692 (2009).
- [44] A. Yamaguchi, N. Shiga, S. Nagano, Y. Li, H. Ishijima, H. Hachisu, M. Kumagai, and T. Ido, *Appl. Phys. Express* **5**, 022701 (2012).
- [45] K. Matsubara, H. Hachisu, Y. Li, S. Nagano, C. Locke, A. Nohgami, M. Kajita, K. Hayasaka, T. Ido, and M. Hosokawa, *Opt. Express* **20**, 22034 (2012).
- [46] D. Akamatsu, H. Inaba, K. Hosaka, M. Yasuda, A. Onae, T. Suzuyama, M. Amemiya, and F. L. Hong, *Appl. Phys. Express* **7**, 012401 (2014).
- [47] T. Tanabe, D. Akamatsu, T. Kobayashi, A. Takamizawa, S. Yanagimachi, T. Ikegami, T. Suzuyama, H. Inaba, S. Okubo, M. Yasuda, F. L. Hong, A. Onae, and K. Hosaka, *J. Phys. Soc. Jpn.* **84**, 115002 (2015).
- [48] Y. G. Lin, Q. Wang, Y. Li, F. Meng, B. K. Lin, E. J. Zang, Z. Sun, F. Fang, T. C. Li, and Z. J. Fang, *Chin. Phys. Lett.* **32**, 090601 (2015).
- [49] R. Hobson, Ph.D. thesis Balliol College, University of Oxford, 2016.
- [50] H. Hachisu, G. Petit, and T. Ido, *Appl. Phys. B* **123**, 34 (2017).
- [51] H. Hachisu, G. Petit, F. Nakagawa, Y. Hanado, and T. Ido, *Opt. Express* **25**, 8511 (2017).
- [52] BIPM Page last updated: 30 November 2018, Recommended values of standard frequencies online at <https://www.bipm.org/en/publications/mises-en-pratique/standard-frequencies>.
- [53] V. A. Dzuba and V. V. Flambaum, *Phys. Rev. D* **95**, 015019 (2017).
- [54] V. V. Flambaum and A. F. Tedesco, *Phys. Rev. C* **73**, 055501 (2006).
- [55] T. H. Dinh, A. Dunning, V. A. Dzuba, and V. V. Flambaum, *Phys. Rev. A* **79**, 054102 (2009).
- [56] J. Lodewyck, S. Bilicki, E. Bookjans, J. L. Robyr, C. Shi, G. Vallet, R. Le Targat, D. Nicolodi, Y. Le Coq, J. Guéna, M. Abgrall, P. Rosenbusch, and S. Bize, *Metrologia* **53**, 1123 (2016).
- [57] M. Pizzocaro, F. Bregolin, P. Barbieri, B. Rauf, F. Levi, and D. Calonico, *Metrologia* **57**, 035007 (2020).
- [58] E. Benkler, B. Lipphardt, T. Puppe, R. Wilk, F. Rohde, and U. Sterr, *Opt. Express* **28**, 15023 (2020).